

Electronic and Steric Structure of Thermal Isomerization Products of 1-Methyltricyclo[4.1.0.0^{2,7}]heptane Radical Cation

V. V. Zverev and V. A. Vasin

Arbuzov Institute of Organic and Physical Chemistry, Kazan Research Center,
Russian Academy of Sciences, Kazan, Tatarstan, Russia

Ogarev Mordovian State University, Saransk, Mordovia, Russia

Received April 6, 2001

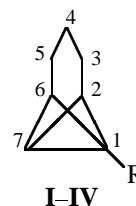
Abstract—Distributions of the positive charge and unpaired electron in stable conformers of the thermal isomerization products of 1-methyltricyclo[4.1.0.0^{2,7}]heptane radical cation, having bicyclo[3.1.1]heptane, bicyclo[4.1.0]heptane, bicyclo[3.2.0]hept-6-ene, and 1,3-cycloheptadiene skeletons, were estimated by the PM3 semiempirical method.

We previously reported [1, 2] on the results of a theoretical study of the structure of radical cations formed from unsubstituted (**I**), 1-methoxycarbonyl- (**II**), and 1-methylthiotricyclo[4.1.0.0^{2,7}]heptane (**III**) by reorganization of the corresponding radical cations in the vertical state A*. In each case, we localized isomers with loose (tricyclic) and completely broken (bicyclic) central C¹–C⁷ bicyclobutane bond in the initial compound (**A** and **B**), bicyclic isomers **C** and **D** with broken side C¹–C² and C²–C⁷ bonds, and monocyclic structures **F** having a 1,3-cycloheptadiene skeleton. In this series, a general trend is successive increase of the relative stability in going from tricyclic systems **A** to monocyclic **F**. An exception is radical cation **IIID** which appears to be less favorable than **IIIA–IIIC** from the viewpoint of energy. The theoretical relative stabilities of radical cations derived from tricycloheptane **I** agree satisfactorily with the experimental data given in [3].

In this work we studied the electronic and steric structure of 1-methyltricyclo[4.1.0.0^{2,7}]heptane (**IV**) radical cations and some products of their thermal isomerization, which can act as reactive intermediates. For example, the anti-Markownikoff addition of nucleophiles (methanol and water) at the central C¹–C⁷ bond of **IV** during photolysis in the presence of 1-cyanonaphthalene as sensitizer was explained by participation of one structural form of the above radical cations. In the absence of nucleophile, radical cation may be involved in further thermal isomerization or disproportionation [4, 5].

First of all, it should be noted that the electronic and steric structure of tricycloheptane **IV** was studied

previously by photoelectron spectroscopy and MINDO/3 quantum-chemical method [6]. Compound **IV** is characterized by a lower ionization potential, 8.20 eV (Table 1; 8.54 eV [7]) against 8.72 eV for **I**, and dipole moment, 0.68 D against 0.84 D for **I**. As in the case of tricycloheptane **I**, geometry optimization of **IV** by the MINDO/3 method gives a structure with planar C²C³C⁴C⁵C⁶ fragment. The C¹–C² and C²–C⁷ bonds become nonequivalent: their lengths are 1.516 and 1.548 Å, respectively, against 1.524 Å in molecule **I**. Simultaneously, the C¹–C⁷ distance increases from 1.501 to 1.514 Å [6].



I, R = H; **II**, R = CO₂Me; **III**, R = SMe; **IV**, R = Me.

We performed calculations of the structure of molecule **IV** by the PM3 method. Unlike MINDO/3, the PM3 procedure predicts puckered structure of the trimethylene bridge in **IV** with a dihedral angle α between the C²C³C⁵C⁶ and C³C⁴C⁵ planes of -140° (*anti* conformer) and 141.3° (*syn* conformer) (Table 1). The same is also typical of compound **I** and tricycloheptanes **II** and **III** [1, 8]. Also, increase in the C¹–C⁷ distance relative to the corresponding distance in **I** (by 0.003 Å) was observed. The heats of formation and the energies of the highest occupied orbitals of the *syn* and *anti* conformers are very similar (Table 1). The highest occupied molecular

Table 1. Heats of formation (ΔH , kJ/mol), geometric parameters, vertical ionization potentials (IP_m , eV), and energies of highest occupied orbitals (ε_m , eV) of tricycloheptane **IV** conformers

Method	Conformer	ΔH	α , deg	l_{17} , Å	$-\varepsilon_1$ (IP_1)	$-\varepsilon_2$ (IP_2)	$-\varepsilon_3$ (IP_3)	$-\varepsilon_4$ (IP_4)
MINDO/3 [6]	Planar	143.4	180	1.514	8.53	9.64	9.87	10.45
PM3	<i>anti</i>	208.6	-140.8	1.480	9.96	10.89	10.91	11.75
	<i>syn</i>	208.7	141.3	1.480	9.97	10.91	10.94	11.67
HF/3-21G	<i>anti</i>	-308.11926 ^a	-136	1.489	9.13	10.67	11.30	11.80
	<i>syn</i>	-308.11894 ^a	136	1.489	9.13	10.65	11.26	11.79
Photoelectron spectroscopy [6]					(8.20)	(9.90)	(10.2)	(10.8)

^a Total energy E , a.u.

orbital (HOMO) in each conformer is localized mainly on the bridgehead carbon atoms C^1 and C^7 (Table 2), which is also characteristic of unsubstituted tricycloheptane **I** [1]. The contribution of C^1 -AO to HOMO of the *anti* conformer is greater than the contribution of C^7 -AO, presumably due to effect of the trimethylene bridge (cf. [1]). The results of PM3 calculations satisfactorily reproduce those obtained for molecule **IV** by nonempirical calculations with the HF/3-21G basis set (Tables 1, 3).

Radical cations of **IV** were also calculated by the PM3 procedure in terms of the unrestricted Hartree–Fock method. Unlike radical cations of the tricycloheptane series studied previously [2], we revealed no local minima for radical cation **IV**, corresponding to structure **A** with loose C^1 – C^7 bond. When geometric parameters of the initial molecule, i.e., of *syn* and *anti* conformers of radical cation **A**^{*}, were used as starting ones, in all cases gradient optimization led to two almost equivalent structures **IVB** having a bicyclo-[3.1.1]heptane skeleton, which corresponds to complete rupture of the C^1 – C^7 bond (Table 4). At fixed C^1 – C^7 bond lengths l_{17} 1.54, 1.60, 1.70, 1.80, and 2.00 Å, the heats of formation of the *syn* conformer are, respectively, 1086.5, 1069.1, 1050.6, 1039.4, and 1023.0 kJ/mol, and those of the *anti* conformer, 1082.9, 1068.2, 1051.2, 1040.6, and 1023.5 kJ/mol. These results prompted us to examine structures **A** and **B** of radical cations derived from **I** and **IV** with the use of higher-level quantum-chemical procedures, restricted open-shell ROHF/3-21G and unrestricted Hartree–Fock procedure UHF/3-31G, as well as of the density functional theory method (DFT). It was somewhat surprising (Table 5) that we failed to reveal a local minimum for structure **IB** in terms of the unrestricted Hartree–Fock procedure with the 3-21G basis set. Even stronger difficulties encountered while calculating radical cations of **IV**. Using the PM3 method, we did not succeed in detecting a local

minimum for structure **A**, while ROHF/3-21G failed to localize structure **B**. Presumably, this is the result of purely mathematical complexity in the development of two minima separated by a small barrier. It is quite probable that both minima could be localized by calculations with basis sets of higher level.

Reorganization of radical cation **IVA**^{*} involving rupture of the side C^1 – C^2 bond leads to bicyclo-[4.1.0]heptane structures **C** which are energetically more favorable than structures **B**. Optimization by the PM3 method gives *chair* and *twist* conformers of **C** (Table 4). The *twist* conformer is more favorable than *chair* by ~11 kJ/mol. Rupture of the side C^2 – C^7 bond gives radical cation **IVD** for which the *chair* conformer is more favorable. It is less stable than radical cations **IVB** and **IVC**. Further reorganization leads to bicyclo[3.2.0]hept-6-ene structures **IVE** which are more stable than **IVB**–**IVD**. Radical cations **IVE** can exist as *cis* and *trans* conformers differing in the position of C^3 and C^6 (C^7) relative to the $C^1C^2C^4C^5$ plane. The *cis* conformer is slightly more stable (Table 4). An analogous pattern is observed for the *cis* ($\Delta H = 1014.3$ kJ/mol) and *trans* conformers ($\Delta H = 1040.3$ kJ/mol) of **IE** which are more stable than radical cations **IA**–**ID** (cf. [2]). Monocyclic radical cation **IVF** having a 1,3-cycloheptadiene skeleton is a product of more profound transformations. It is more favorable than bicyclic radical cations **IVB**–**IVE** by 89.1 to 197.7 kJ/mol (Table 4).

The data in Table 2 show distribution of the effective charge (q) and spin populations (s) in radical cations **A**^{*} and **B**–**F** of hydrocarbon **IV**, according to PM3 calculations. The probabilities for unpaired electron to be localized at the bridgehead C^1 and C^7 atoms of radical cation **A**^{*} are approximately similar and are greater than those calculated for the other carbon atoms. On the other hand, a small positive charge is localized on C^7 , while its main part resides on hydrogen atoms (cf. [9]). The unpaired electron in structures

Table 2. Effective charges on atoms (q), atom populations in the HOMO (p), and atom spin populations (s) in the molecule of tricycloheptane **IV** and radical cations **IE** and **IVA*–F**, calculated by the PM3 method

Atom	IE (<i>trans</i>)		IE (<i>cis</i>)		IV (<i>anti</i>)		IV (<i>syn</i>)		IVA* (<i>anti</i>)	
	q	s	q	s	q	p^a	q	p^a	q	s
C ¹	0.187	0.411	–0.132	–0.035	–0.192	0.631	–0.180	0.595	0.001	0.438
C ²	–0.160	–0.046	–0.070	0.032	–0.047	0.119	–0.046	0.118	–0.040	–0.041
C ³	–0.052	0.057	–0.116	0.000	–0.079	0.136	0.078	0.136	–0.050	0.090
C ⁴	–0.160	–0.047	–0.070	0.032	–0.090	0.019	–0.090	0.019	–0.124	–0.014
C ⁵	0.187	0.401	–0.132	–0.035	–0.079	0.136	–0.078	0.136	–0.051	0.096
C ⁶	–0.132	–0.011	0.184	0.352	–0.046	0.119	–0.047	0.118	–0.039	–0.040
C ⁷	–0.132	–0.011	0.184	0.352	–0.201	0.584	–0.213	0.622	0.037	0.435

Atom	IVB (<i>anti</i>)		IVB (<i>syn</i>)		IVC (<i>chair</i>)		IVC (<i>twist</i>)	
	q	s	q	s	q	s	q	s
C ¹	0.376	0.032	0.393	–0.018	–0.305	–0.053	–0.290	–0.086
C ²	–0.105	–0.104	–0.104	–0.102	0.414	0.013	0.355	0.041
C ³	–0.069	0.039	–0.072	0.044	–0.187	0.001	–0.180	–0.006
C ⁴	–0.131	–0.007	–0.139	0.073	–0.086	–0.005	–0.107	–0.004
C ⁵	–0.069	0.039	–0.071	0.044	–0.096	0.037	–0.113	0.047
C ⁶	–0.105	–0.104	–0.107	–0.102	0.022	–0.095	0.069	–0.106
C ⁷	–0.170	1.161	–0.178	1.161	–0.046	1.045	–0.069	1.060

Atom	IVD (<i>chair</i>)		IVE (<i>trans</i>)		IVE (<i>cis</i>)		IVF	
	q	s	q	s	q	s	q	s
C ¹	–0.272	–0.060	–0.113	–0.053	–0.113	–0.051	0.072	0.635
C ²	0.398	0.004	–0.073	0.036	–0.075	0.034	0.086	0.018
C ³	–0.187	0.001	–0.104	–0.001	–0.113	–0.001	–0.117	0.080
C ⁴	–0.076	–0.006	–0.074	0.021	–0.076	0.020	0.135	0.457
C ⁵	–0.106	0.045	–0.119	–0.025	–0.117	–0.024	–0.134	–0.041
C ⁶	0.058	–0.112	0.186	0.341	0.186	0.235	–0.100	0.016
C ⁷	–0.063	1.139	0.125	0.642	0.122	0.481	–0.123	–0.058

^a $\Sigma p_m = 2$.**Table 3.** Charges on atoms (q), atom populations of the HOMO (p), spin densities on atoms (ρ), and free valence indices (f) for *anti* conformers of radical cations **IA**, **IB**, and **IVA** and molecule **IV**

Atom	IA (ROHF/3-31G)				IB (ROHF/3-31G)				IA (UHF/3-31G)			
	q	s	ρ	f	q	s	ρ	f	q	s	ρ	f
C ¹	–0.143	0.631	0.081	0.398	–0.044	0.943	0.133	0.890	–0.082	0.737	0.187	0.328
C ^{2,6}	–0.329	0.016	0.000	0.000	–0.460	0.000	0.005	0.000	–0.339	–0.283	–0.079	0.024
C ^{3,5}	–0.365	0.044	0.022	0.002	–0.355	0.014	0.012	0.000	–0.362	0.137	0.047	0.012
C ⁴	–0.450	0.004	0.000	0.000	–0.486	0.014	0.000	0.000	–0.045	–0.028	–0.011	0.000
C ⁷	–0.039	0.219	0.082	0.082	0.161	0.007	0.002	0.000	–0.074	0.649	0.151	0.243

Table 3. (Contd.)

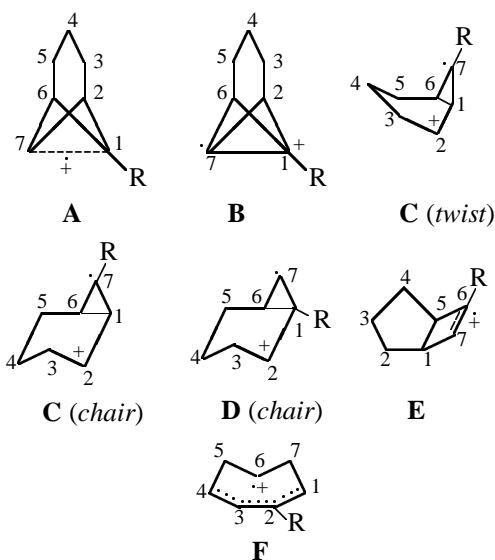
Atom	IA (DFT)		IB (DFT)		IV (HF/3-21)		IVA (ROHF/3-21)			
	<i>q</i>	<i>s</i>	<i>q</i>	<i>s</i>	<i>q</i>	<i>p</i>	<i>q</i>	<i>s</i>	ρ	<i>f</i>
C ¹	0.025	0.060	0.095	0.388	-0.258	0.611	0.150	0.193	0.019	0.037
C ^{2,6}	-0.012	0.099	0.008	0.026	-0.175	0.119	-0.322	0.010	0.000	0.000
C ^{3,5}	-0.036	0.026	0.007	-0.003	-0.396	0.161	-0.356	0.040	0.023	0.002
C ⁴	0.091	0.321	-0.042	0.007	-0.408	0.026	-0.454	0.004	0.002	0.000
C ⁷	0.081	0.215	0.077	0.482	-0.092	0.590	-0.134	0.667	0.060	0.004

Table 4. Heats of formation (ΔH , kJ/mol) and relative energies (ΔE , kJ/mol) of radical cations derived from tricycloheptane **IV**, calculated by the PM3 method

Structure	ΔH	ΔE
A * (<i>anti</i>)	1129.2	109.0
B (<i>syn</i>)	1021.2	1.0
B (<i>anti</i>)	1020.2	0.0
C (<i>chair</i>)	1009.9	-10.4
C (<i>twist</i>)	998.9	-21.3
D (<i>chair</i>)	1036.4	16.2
E (<i>trans</i>)	932.3	-88.0
E (<i>cis</i>)	927.8	-92.4
F	834.5	-181.5

Table 5. Total energies (*E*, a.u.) and geometric parameters of *anti* conformers of radical cations **A** and **B** derived from hydrocarbons **I** and **IV**, calculated *ab initio* and by the DFT method

Method	Radical cation	$-E$	l_{17} , Å	$-\alpha$, deg
ROHF/3-21	IA	269.02743	1.738	137
	IB	269.00790	2.038	147
	IVA	307.86545	1.797	134
UHF/3-21	IA	269.03569	1.752	138
DFT/3Z	IA	272.12084	1.638	138
	IB	272.07555	2.069	146



B is localized on C⁷, and the positive charge, on the C¹ atom which is neighboring to the methyl group. A specific structural feature of bicyclic radical cations **C** and **D** is that the largest effective positive charge therein is localized on C² while the unpaired electron is most likely to occur on C⁷. The positive charge in

structures **E** is localized mainly on C⁶ and C⁷, the charge on C⁶ being larger. The same atoms contribute most to the spin population. The probability for unpaired electron to occur on C⁷ is almost twice as high as on C⁶. The largest contribution to spin population in radical cation **F** is given by C¹ and C⁴, and the positive charge in **F** is localized on C¹, C², and C⁴.

The charge distributions, atom spin populations, spin densities on atoms (ρ), and free valence indices (*f*) in the *anti* conformer of radical cation **IVA**, calculated by the ROHF/3-21G method, are collected in Table 3. For comparison, analogous data for the *anti* conformers of **IA** and **IB**, obtained *ab initio* and by the DFT method, are also given. On the whole, these data reproduce general trends in the charge distribution and atom spin populations, determined for the same isomers by the PM3 method [2]. Radical cations **IA** and **IB** may be intermediates in photosensitized nucleophile addition at the C¹–C⁷ bond of substrate **I** [5]. However, taking into account high degree of symmetry of the substrate, the above data did not allow us to conclude unambiguously which step, heterolytic or homolytic, follows one-electron transfer. If this step is nucleophilic attack, it will occur at the carbon

atom bearing the maximal positive charge. In the case of homolytic reaction, carbon atom possessing the largest index of free valence should be involved [10]. In both cases, similar products will be formed from compound **I**. On the other hand, the results of PM3 calculations and the assumption that one-electron transfer from the central C¹–C⁷ bond is followed by heterolytic reaction do not explain formation of anti-Markownikoff adducts in sensitized photolysis of compound **IV** with nucleophiles [4, 5] by participation of radical cation **B** as intermediate, for distribution of the positive charge therein is unfavorable for this process. According to the data of Table 3, radical cation **IVA** cannot be intermediate for the same reason provided that the regioselectivity is charge-controlled. Probably, the reaction with nucleophile occurs in an earlier step of transformations involving radical cations whose structure approaches that of state A*. By contrast, the assumption that one-electron transfer is followed by radical rather than ionic reaction is well consistent with the free valence indices found for radical cations **IVA**. Such reaction occurs at the C¹ atom which is characterized by the maximal index. Next follows addition of a nucleophile to C⁷, leading to anti-Markownikoff adduct with a bicyclo-[3.1.1]heptane structure. Undoubtedly, in order to better understand specificity of reactions of tricyclo-[4.1.0.0^{2,7}]heptane radical cations, their theoretical and experimental studies must be continued.

EXPERIMENTAL

The PM3 calculations (for radical cations, by the unrestricted Hartree–Fock method) were performed with the original parametrizations [11, 12] using MOPAC 6.0 software package [13]. Secondary derivative matrix was calculated for stationary points. The average values of the $\langle S^2 \rangle$ operator did not exceed 0.77; this value is very close to 0.750, which corresponds to the doublet state with $S = 1/2$. Therefore, the contribution of the quartet state with $S = 3/2$ for the structures under study is small. Nonempirical calculations were performed using GAMESS program [14]. DFT calculations with PBE exchange–correlation functional and TZ2P extended basis set were performed using PRIRODA 1.4 program [15].

ACKNOWLEDGMENTS

This study was financially supported by the Ministry of Education of the Russian Federation (project no. E00-5.0-30).

REFERENCES

1. Zverev, V.V. and Vasin, V.A., *Zh. Obshch. Khim.*, 1998, vol. 68, no. 11, p. 1908.
2. Zverev, V.V. and Vasin, V.A., *Zh. Obshch. Khim.*, 2000, vol. 70, no. 6, p. 987.
3. Arnold, A., Burger, U., Gerson, F., Kloster-Jensen, E., and Schmidlin, S.P., *J. Am. Chem. Soc.*, 1993, vol. 115, no. 10, p. 4271.
4. Gassman, P.G. and Olson, K.D., *J. Am. Chem. Soc.*, 1982, vol. 104, no. 13, p. 3740.
5. Gassman, P.G. and Carrol, G.T., *Tetrahedron*, 1986, vol. 42, no. 22, p. 6201.
6. Bischof, P., Gleiter, R., Taylor, R.T., Browne, A.R., and Paquette, L.A., *J. Org. Chem.*, 1978, vol. 43, no. 12, p. 2391.
7. Schloßer, A., Philipp, F., Mickler, W., Szeimies, G., and Martin, H.-D., *Chem. Ber.*, 1980, vol. 113, no. 3, p. 1053.
8. Zverev, V.V. and Vasin, V.A., *Zh. Obshch. Khim.*, 1999, vol. 69, no. 7, p. 1188.
9. Wiberg, K.B., Schleyer, P.v.R., and Streitwieser, A., *Can. J. Chem.*, 1996, vol. 74, no. 6, p. 892.
10. Higashi, K., Baba, H., and Rembaum, A., *Quantum Organic Chemistry*, New York: Interscience, 1965. Translated under the title *Kvantovaya organicheskaya khimiya*, Moscow: Mir, 1967, p. 16.
11. Dewar, M.J.S. and Thiel, W., *J. Am. Chem. Soc.*, 1977, vol. 99, no. 15, p. 4899.
12. Stewart, J.J.P., *J. Comput. Chem.*, 1989, vol. 10, no. 2, p. 209.
13. Stewart, J.J.P., *J. Comput. Aided Mol. Design*, 1990, vol. 4, no. 1, p. 1.
14. Schmidt, M.W., Baldridge, K.K., Boatz, J.A., Elbert, S.T., Gordon, M.S., Jensen, J.H., Koseki, S., Matsunaga, N., Nguyen, K.A., Su, S.J., Windus, T.L., Dupuis, M., and Montgomery, J.A., *J. Comput. Chem.*, 1993, vol. 14, no. 7, p. 1347.
15. Laikov, D.N., *Chem. Phys. Lett.*, 1997, vol. 281, p. 151.